
REPRESENTATION LEARNING USING A SINGLE FORWARD PASS

A PREPRINT

 **Aditya Somasundaram***

Department of Electrical Engineering
IIT Hyderabad
ee20btech11002@iith.ac.in

 **Pushkal Mishra***

Department of Electrical Engineering
IIT Hyderabad
ee20btech11042@iith.ac.in

 **Ayon Borthakur**

Mehta Family School of Data Science & Artificial Intelligence
IIT Guwahati
ayon.borthakur@iitg.ac.in

February 16, 2024

ABSTRACT

We propose a neuroscience-inspired **Solo Pass Embedded Learning Algorithm (SPELA)**. SPELA is a prime candidate for training and inference applications in Edge AI devices. At the same time, SPELA can optimally cater to the need for a framework to study perceptual representation learning and formation. SPELA has distinctive features such as neural priors (in the form of embedded vectors), no weight transport, no update locking of weights, complete local Hebbian learning, single forward pass with no storage of activations, and single weight update per sample. Juxtaposed with traditional approaches, SPELA operates without the need for backpropagation. We show that our algorithm can perform nonlinear classification on a noisy boolean operation dataset. Additionally, we exhibit high performance using SPELA across MNIST, KMNIST, and Fashion MNIST. Lastly, we show the few-shot and 1-epoch learning capabilities of SPELA on MNIST, KMNIST, and Fashion MNIST, where it consistently outperforms backpropagation.

1 Introduction

Perceptual representation learning (Sucholutsky et al. [2023]) of external world information never occurs in a randomly initialized state of the brain. Instead, this external world information is merged with pre-existing knowledge (**priors**) in the brain (Summerfield and Koechlin [2008], Binder et al. [2009], Wang and Morris [2010], Kok et al. [2013], Hardstone et al. [2021], Brod et al. [2013]). To support this claim, there exists a large body of work including behavioral and systems neuroscience studies. Through behavioral experiments, Piaget [1929] showed that world knowledge is essential for memory construction; Craik and Lockhart [1972] showed that memory is a function of the degree of integration with priors, and Bransford and Johnson [1972] observed improved comprehension of prose with prior knowledge. Moreover, Kumaran et al. [2009, 2012] noticed that brain regions such as the medial prefrontal cortex (mPFC), the hippocampus, and the posterior cingulate cortex contribute to the prior generation; van Kesteren et al. [2010], van Kesteren et al. [2013] observed that mPFC mediates integration of information similar to prior knowledge. Despite extensive research, we still lack a mechanistic understanding of this interaction of real-world stimuli and previous knowledge (priors) that can help in understanding representation formation (Brod et al. [2013]).

Similarly, the current backpropagation-trained network (deep neural networks) starts with a random initialization (Narkhede et al. [2022]) and hence lacks such integration of prior knowledge. Moreover, presently popular deep neural networks update parameters in the network during training to improve performance (credit assignment) in a manner that is not biologically plausible (Bengio et al. [2016], Lillicrap et al. [2016], Richards et al. [2019]). For

*AS and PM are first authors with equal contributions. Authorship order is determined by a coin toss. AB is the senior author.

instance, during parameter updates, gradients are propagated backward recursively which implies that parameter updates of a layer are dependent on all backward layers (global learning problem) (Whittington and Bogacz [2019]). During the backward pass, exact (transposed) weights of the forward pass and activation information are utilized for parameter updates (weight transport problem) (Lillicrap et al. [2014], Akrouf et al. [2019]). Adding to it, for every forward pass, a backward pass needs to be computed (with forward pass updates frozen), which prevents the online utilization of inputs (update locking problem) (Czarnecki et al. [2017], Jaderberg et al. [2017]).

These limitations make a deep neural network trained with backpropagation (LeCun et al. [2015]) unsuitable for understanding the perceptual representation learning and formation in the brain as well as for training (and inference) of the networks in resource-constrained edge AI devices. Considering these requirements, we here introduce SPELA, which has a unique set of characteristics. More precisely,

- (a) SPELA offers a framework to integrate the external world information (input data) with prior knowledge or neural priors (in the form of embedded vectors).
- (b) SPELA supports a complete local Hebbian learning (Hebb [1949]) for credit assignment. During inference, only the final layer output is sufficient for prediction.
- (c) It uses a single forward pass (with no backward pass) for weight update and inference. Hence, provides a no-weight transport solution.
- (d) SPELA also doesn't require update locking of weights.
- (e) It requires no hidden layer and only 1 output layer with 2 neurons to solve the non-linear XOR classification.
- (f) Empirical results show that SPELA easily outperforms an equivalent backpropagation-trained network under a single-epoch training regime.
- (g) The speed-accuracy tradeoff (SAT; Heitz [2014], Penconek [2022], Zimmerman [2011]) is a hallmark of living organisms with reasonably simple neural circuitry such as insects, and also for humans who possess very complex neural circuitry. However, the neural mechanisms mediating SAT are not very clear. SPELA, owing to its unique characteristic of enabling predictions at every layer within the network (not known to be present in traditional neural networks), presents a natural platform for investigating the mechanisms associated with SAT.
- (h) Its neuroscience-inspired design makes it a prime candidate for studying perceptual learning mechanisms in the brain.
- (i) Finally, SPELA does not require neuron bias and does not need to store forward activations for future use. All of these properties, make SPELA also useful for edge AI devices.

We believe this approach can pave the way toward the realization of the next generation of neuroscience-inspired AI systems (Zador et al. [2023]). Furthermore, this work can also help guide the development of future neuromorphic systems with on-chip learning capabilities (Davies et al. [2018], Modha et al. [2023]).

1.1 Background Works

Hinton [2022] presents the Forward-Forward (FF) algorithm for neural network learning, replacing backpropagation with two forward passes: one with positive (real) data and the other with generated negative data. Each layer aims to optimize a "goodness metric" for positive data and minimize it for negative data. Separating positive and negative passes in time enables offline processing, facilitating image pipelining without activity storage or derivative propagation interruptions. In contrast to Hinton's approach, which aggregates goodness values across layers, SPELA is capable of performing classification at any layer without the need for storing "goodness" memory. Furthermore, unlike FF, SPELA eliminates the necessity for generating separate negative data for training. Instead, it efficiently utilizes available data without requiring additional processing. Hinton's work has also been extended to spiking neural networks using contrastive signal-dependent plasticity (Ororbia [2023]) by processing sensory input over a stimulus window. It is worth mentioning here that although spikes make major contributions to computations in the brain, work by Gidon et al. [2020] establishes the necessity to take into account the contributions of graded activities too. Similarly, the recently designed neuromorphic chip Loihi 2 Orchard et al. [2021] also introduces graded spiking neurons. Using a forward and a backward pass, Pehlevan [2019] introduces the concept of non-negative similarity matching cost function for spiking neural networks to exhibit local learning and therefore enable the effective use of neuromorphic hardware. Lansdell et al. [2020] introduces a hybrid learning approach wherein each neuron learns to approximate the gradients. The learning feedback weights provide a biologically plausible way of achieving good performance as compared to backpropagation-based trained networks. Giampaolo et al. [2023] follows a similar strategy to our approach of dividing the entire network into sub-networks and training them locally using backpropagation (SPELA divides the network into sequential layers). In section 3.4, we delve into a

straightforward and biologically plausible few-shot learning neural mechanism proposed by Sorscher et al. [2022a]. To the best of our knowledge, none of the previous works focus on using neural priors (in the form of embedded vectors) along with features such as a single forward pass without the need for any backward pass during credit assignment (see 1 for details).

2 Methods

2.1 Network Initialization and Learning Methods

The network is defined as follows: there are L layers, each containing l_i neurons. The weights of the network are initialized at random. Each layer L_i (except the input layer) has N (number of classes in the dataset given) number of symmetric vectors, each of dimension l_i . These symmetric vectors are assigned a unique class. As the activation vector is also in the l_i dimensional space, we can measure how close the activation vector points to a particular symmetric vector using a simple cosine similarity function (Momeni et al. [2023]). The network outputs the class assigned to the symmetric vector which is closest to the activation vector in terms of cosine similarity. These symmetric vectors remain fixed and are not updated during training.

Arranging the vector embeddings When embedding vectors in any space, it is instinctive to allocate an equal portion of the space to each vector or class. Consequently, arranging these embeddings symmetrically provides an elegant solution.

In the first layer, N symmetric vectors of dimension l_1 are generated and are assigned a unique class at random. To maintain relative positions of these symmetric vectors across subsequent layers, multidimensional scaling (MDS) (Kruskal [1964]) is used to transform the vectors from dimension l_i to l_{i+1} as depicted in Fig. 1.

Remark. *The symmetric vectors in the n^{th} dimension are generated by simulating the physics of electrons in the n^{th} dimension by restricting them on the unit norm ball until the electrostatic energy converges sufficiently (Saff and Kuijlaars [1997], Cohn and Kumar [2007]).*

Training: (Algorithm 1) Given data x and label y , the network learns locally by minimizing the cosine similarity loss between the activation vector (arising from input x) and the symmetric vector (which is assigned the class y). There is no restriction on batch size (both training and testing); multiple data points can be given before the weight update. Using this training method, the weights of the layers are updated sequentially. Since our training occurs in a layer-wise manner, SPELA can be easily extended to accommodate multiple layers. As mentioned in the introduction, this training method aligns perfectly with the Hebbian learning principle (Hebb [1949]).

Algorithm 1 Training MLP with SPELA

```

1: Given: An input ( $X$ ), label ( $y$ ), number of layers ( $K$ ) and number of epochs ( $E$ )
2: Define:  $\text{cos\_sim}(A, B) = \frac{A \cdot B}{\|A\| \cdot \|B\|}$ 
3: Set:  $h_0 = x$ 
4: for  $k \leftarrow 1$  to  $K$  do ▷ Iterate through layers
5:   for  $e \leftarrow 1$  to  $E$  do ▷ Iterate through epochs
6:      $h_k = \sigma_k(W_k h_{k-1} + b_k)$ 
7:      $\text{loss} = \log(2 - \text{cos\_sim}(h_k, \text{vecs}_k(y)))$  ▷  $\text{vecs}_k(\cdot)$  is the set of symmetric vectors
8:      $W_k \leftarrow W_k - \alpha * \Delta_{W_k}(\text{loss})$  ▷ Weight update using local loss
9:   end for
10: end for

```

Inference: (Algorithm 2) Given data x , the network measures how close each symmetric vector is to the activation vector (arising from input x) and declares the closest symmetric vector as the winner. The prediction is the class assigned to the winning symmetric vector as shown in Fig. 2.

Speed accuracy tradeoff: SPELA can naturally aid in the understanding of the SAT mechanisms. This phenomenon can be ascribed to the characteristics of SPELA, where classification occurs at each layer. As the number of layers increases, i.e., the network deepens, a greater number of nonlinearities are applied to enhance the classification process. In other words, if there is a time constraint, predictions can be extracted from earlier layers with less accuracy but if given more time, more accurate predictions can be made from the end layers.

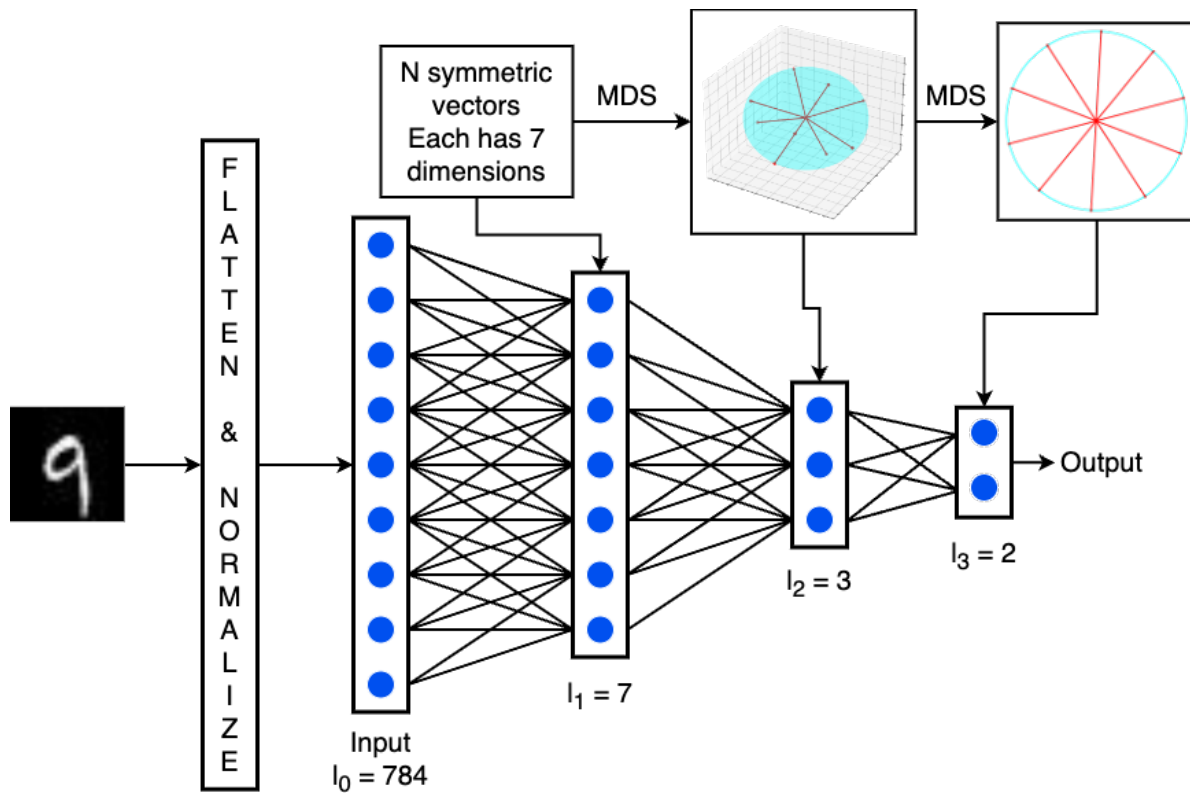


Figure 1: Network Architecture: The illustrations provided depict the structure of the network. It's important to recognize that each layer possesses a distinct set of symmetric vectors within varying dimensional spaces. In the given instance, the network is trained with the MNIST dataset, resulting in 10 symmetric vectors for each layer.

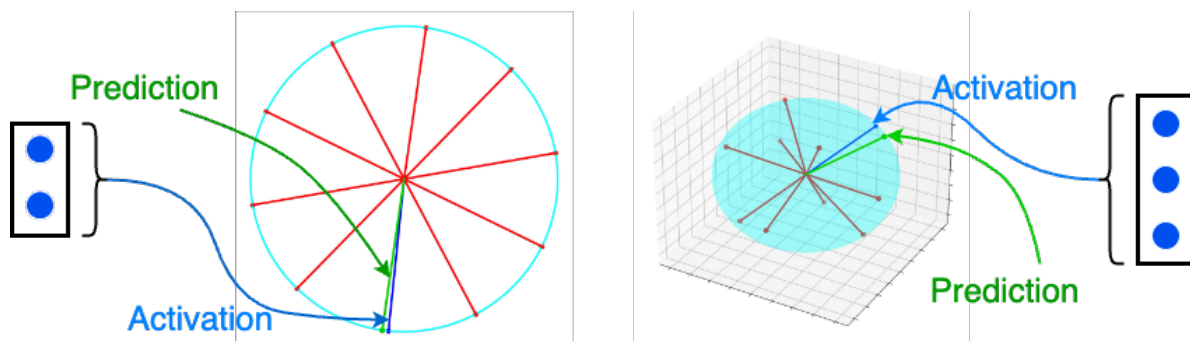


Figure 2: Prediction Method: The inference is conducted by evaluating the closeness in direction between the activation vector and the symmetric vectors. The activation vector is represented in blue and the prediction is in green.

Algorithm 2 Inference on MLP trained with SPELA

```

1: Given: An input (X)
2: Define:  $\text{cos\_sim}(A, B) = \frac{A \cdot B}{\|A\| \cdot \|B\|}$ 
3: Set:  $h_0 = x$ 
4: for  $k \leftarrow 1$  to  $K$  do                                     ▷ Passing data through all the layers
5:    $h_k = \sigma_k(W_k h_{k-1} + b_k)$ 
6: end for
7: for  $i \leftarrow 1$  to  $N$  do                                     ▷ N is the number of classes
8:    $S_i = \text{cos\_sim}(h_K, \text{vecs}(i))$                              ▷ Similarity between activation vector and symmetric vectors
9: end for
10: Prediction:  $\text{argmax}_i S_i$                                    ▷ Class corresponding to the maximum score is prediction

```

2.2 Negating the necessity of bias

At every layer, we apply a linearity \mathbf{W} , followed by a non-linearity σ . The loss function measures how close the activation vector \mathbf{h} is to the preset vectors \mathbf{s} . There will exist a projection \mathbf{R} of the input \mathbf{x} (assuming \mathbf{x} is non zero) such that $\mathbf{R}\mathbf{x}$ makes the same angle as $\sigma(\mathbf{W}\mathbf{x} + \mathbf{b})$ makes with \mathbf{s} . Introducing a bias term would expedite the learning process by increasing the number of parameters, but it is not essential in SPELA. This is also illustrated in sections 3.2 and 3.4, where we conduct experiments while configuring the bias in the networks to be zero.

Note that **if bias is not given** in the network, the non-linearities applied must allow negative values as the activation vectors must be allowed to move throughout the n dimensional space (the ReLU unit will not work but LeakyReLU will). Table 1 presents contrasts between SPELA and other learning algorithms. SPELA exhibits the most favorable traits.

Learning Methods	BP	FF	PEP	MPE	SPELA
Forward Pass	1	2	2	3	1
Backward Pass	1	0	0	0	0
Weight Update	1	2	1	1	1
Loss function	global	local	global	global	local
Activations	all	current	all	current	current

Table 1: Different learning algorithms are compared and contrasted with SPELA. PEP stands for PEPITA (Dellaferrera and Kreiman [2022]) and MPE for MEMPEPITA (Pau and Aymone [2023]). FF and SPELA algorithms have a local loss function for each layer, while in BP (LeCun et al. [2015]), PEP, and MPE the loss function is computed at the output layer. FF, MPE, and SPELA need to store only activation buffers for the current layers while BP and PEP are for all layers.

3 Results**3.1 Experiments on boolean operations****3.1.1 Noisy Boolean Dataset as the First Step**

It is well known that a multilayer perceptron network with non-linear activation after being trained with back-propagation can solve the linearly inseparable XOR problem. Biological neural circuits on the other hand have various types of nonlinearities and hence should be able to solve the XOR problem in multiple ways. In fact, Gidon et al. [2020] showed that the pyramidal neuron dendrites can solve this problem using a variant of graded action potentials (dCaAPs). Moreover, Noel et al. [2023] showed that a small network with a biologically plausible oscillating activation function can also classify nonlinear data; Kim et al. [2022] proposed a multi-perceptron model of cortical neurons for solving the soft XOR problem.

3.1.2 Findings of SPELA on Noisy Boolean Dataset

Motivated by these studies, we evaluate SPELA against backpropagation to determine its relative performance on a synthetically generated dataset involving noisy boolean operations. The network (SPELA) has 2 layers (including an input layer) with 2 input neurons, 2 output neurons, and a non-linearity $f(x) = |x|$. Averaged over 10 trials, the algorithm achieves 100% accuracy as depicted in Table 2. SPELA, in this design, has a bias; it achieves the 100%

accuracy in 20 epochs using 200 data samples with a test-to-train split of 10 : 90; batch size of 1, and a learning rate of 0.01. The samples in the synthetic boolean dataset are imbued with Gaussian noise $\mathcal{N}(0, 0.01)$. For the same noisy boolean dataset, an equivalent backpropagation-trained network has 3 layers with 2 (input layer), 3, and 2 neurons. All layers have bias. It is trained on 200 samples with a test-to-train split of 10 : 90 imbued with Gaussian noise $\mathcal{N}(0, 0.01)$ and batched into sizes of 1; for 10 epochs and with a learning rate of 0.01.

Operation	Train Accuracy		Test Accuracy	
	SPELA	Backprop	SPELA	Backprop
AND	100%	100%	100%	100%
OR	100%	100%	100%	100%
XOR	100%	100%	100%	100%

Table 2: Training and testing performance of SPELA against an equivalent backpropagation trained network on the noisy boolean operations dataset.

Compared to traditional backpropagation, SPELA requires no hidden layer and only a single output layer to solve the nonlinear classification problem of XOR. Furthermore, it requires only 2 neurons while a backpropagation-trained network has been shown to need more neurons. As shown in Fig. 3 the loss emerging from SPELA also converges rapidly.

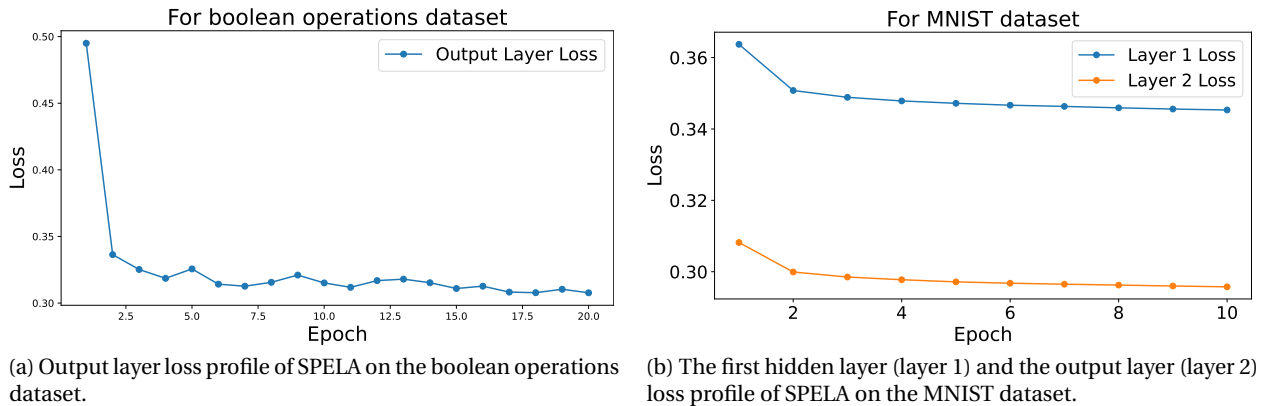


Figure 3: The loss versus epoch number profile emerging from SPELA for both the boolean operations dataset and the MNIST dataset.

3.2 Experiments on MNIST, KMNIST, and Fashion MNIST datasets

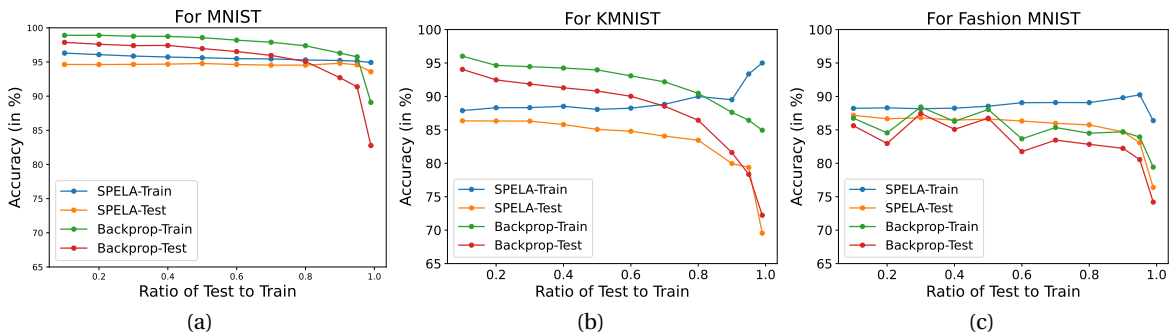


Figure 4: The classification accuracy (averaged over 3 trials) of the equivalent multi-layer networks trained using SPELA and backpropagation for different test-to-train ratios of MNIST, KMNIST, and Fashion MNIST datasets is juxtaposed. Note that the classification accuracy of SPELA remains consistent up to a ratio of approximately 0.6, whereas, for backpropagation, it decreases steadily with an increase in ratio.

Staying within the realm of biological plausibility, we test the generalization capacity of SPELA. Following the previous success of a moth olfaction-inspired network (Delahunt and Kutz [2019]) as well by a multi-compartment neuron model (with dendritic architecture; Jones and Kording [2020]), we select MNIST. In addition, we use harder versions of it, namely the KMNIST and Fashion MNIST datasets.

Figures 4a, 4b, and 4c show accuracy vs test-to-train ratio on MNIST, KMNIST, and Fashion MNIST respectively using SPELA and backpropagation. The network (SPELA) has 3 layers containing 784, 300, and 20 neurons. It has been trained for 10 epochs on a batch size of 64, with a learning rate of 0.001 and **no bias**. For backpropagation, the network also has 3 layers and contains 784, 300, and 10 neurons. It has bias and is trained for 10 epochs on a batch size of 64, with a learning rate of 0.001. From Fig. 4, we observe that SPELA can easily compete with a backpropagation-trained network in classification accuracy. When the bias is set to zero, SPELA's performance exceeds that of a backpropagation-trained network.

3.3 T-SNE plots for better visual understanding of representations

To get a better understanding of the representations of MNIST, KMNIST, and Fashion MNIST formed by SPELA versus a backpropagation-trained network, t-SNE plots have been depicted in figures 5 and 6. The plots exhibit a striking resemblance despite the algorithmic differences, and the class-specific cluster formation is easily noticeable.

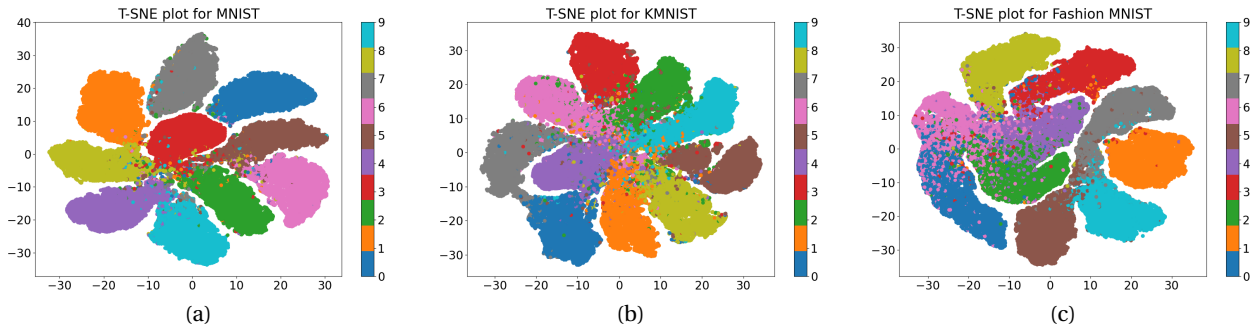


Figure 5: t-SNE plots for a multi-layer neural network trained using SPELA.

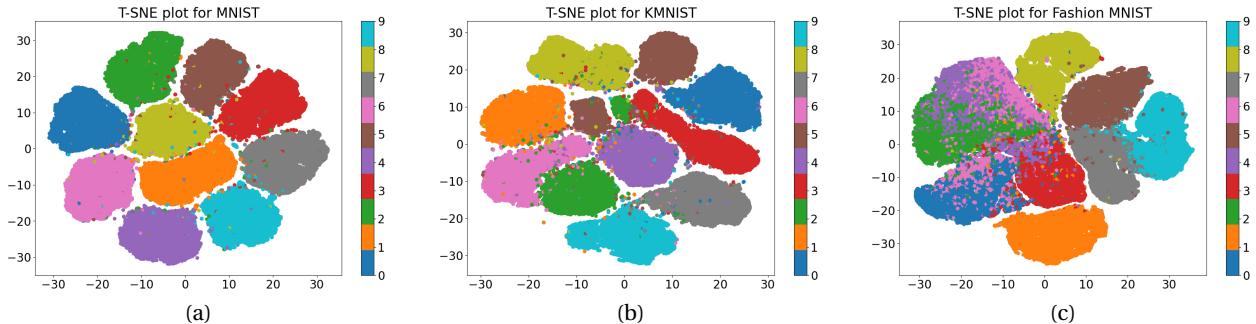


Figure 6: t-SNE plots for a multi-layer neural network trained using backpropagation.

For obtaining the t-SNE plots, the networks have been trained as mentioned. The network (SPELA) has 3 layers each containing 784, 300, and 20 neurons; with no bias. It has been trained for 15 epochs with a learning rate of 0.001 on data batched into sizes of 64. The traditional backpropagation network has 3 layers each containing 784, 300, and 10 neurons; with bias. It has been trained for 10 epochs with a learning rate of 0.001 on data batched into sizes of 64. The test-to-train split is 10 : 90 for both networks.

3.4 Probing into Few-Shot Few Epoch Learning capabilities of SPELA

3.4.1 The necessity for exploring few-shot few epoch learning of SPELA

Despite significant progress in the field of neural networks, these networks still are unable to match the human-level performance of learning from a few exposures (Smith et al. [2002], Quinn et al. [1993], Rastogi [2022]). There exists

a rich resource of work and interest in human-like few-shot learning (Lake et al. [2015], Cao et al. [2021], Sorscher et al. [2022b]). It is worth mentioning at this point that in human learning, one cannot expect the *training data* to be available for multiple instances of presentations (multiple epochs). Human learning is both single / few-shot and single / few epoch(s).

Due to its significantly greater biological plausibility, aligning more closely with human learning processes, it becomes imperative to explore the few-shot single-epoch learning capabilities of SPELA. The rapid convergence of the loss function (Fig. 3) begs the same question as well.

3.4.2 Findings of few-shot few epoch learning experiments

Experiments to train a network using SPELA using only a single epoch on MNIST, KMNIST, and Fashion MNIST are conducted and results are presented in Fig. 7. The network (SPELA) has 5 layers containing 784, 200, 100, 50, and 15 neurons. Here, SPELA has no bias; employs a learning rate of 0.005 and a batch size of 64. Moreover, when the test-to-train ratio is very high (in the regime of 0.95, 0.99) SPELA performs significantly better than backpropagation (see Table 3). The equivalent backpropagation trained network has 5 layers containing 784, 200, 100, 50, and 10 neurons. It has bias; employs a learning rate of 0.001 and has a batch size of 64. SPELA’s efficiency in learning features with minimal data points and epochs and with no neuron bias is underscored.

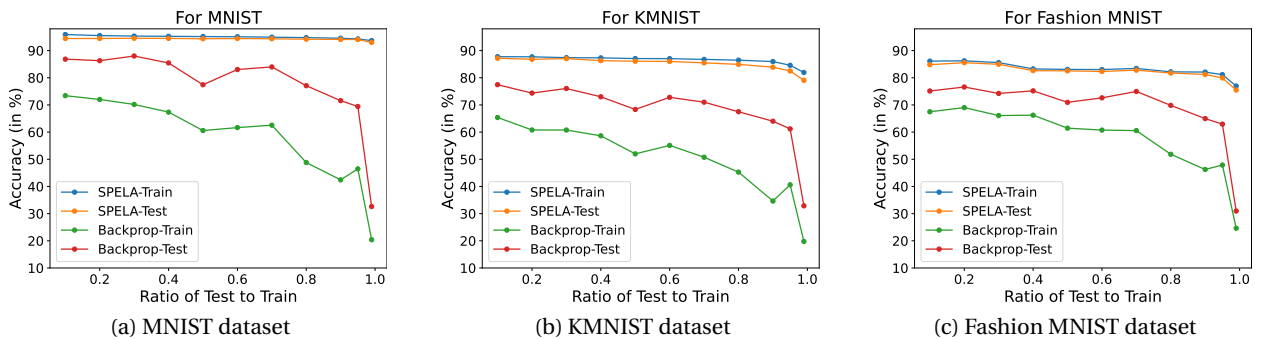


Figure 7: Accuracy vs test-to-train ratio for **1 epoch** using both SPELA and backpropagation on MNIST, KMNIST, and Fashion MNIST datasets. Observe that at very high test-to-train ratios, backpropagation performs much worse than SPELA (see Table 3).

Test-to-train ratio	Dataset	Mean \pm Std. Dev.(in %)	
		SPELA (1 epoch)	Backprop (1 epoch)
0.95	MNIST	94.07 ± 0.29	69.43 ± 4.89
0.99		92.99 ± 0.19	32.61 ± 6.01
0.95	KMNIST	82.50 ± 0.71	61.18 ± 1.42
0.99		79.06 ± 0.78	32.86 ± 5.39
0.95	Fashion MNIST	79.93 ± 3.58	62.94 ± 6.74
0.99		75.48 ± 2.89	30.96 ± 8.88

Table 3: The **few-shot 1 epoch** learning capabilities of SPELA are put forth. The mean and standard deviations on accuracies obtained during the classification of MNIST, KMNIST, and Fashion MNIST for high test-to-train ratios with SPELA and backpropagation (both trained for 1 epoch) are compared.

4 Conclusion

SPELA is a novel and revolutionary idea to train machine learning models without the need for backpropagation. It’s both biologically plausible and computationally efficient. It has a **unique combination** of features such as no weight transport (Bengio et al. [2016], Lillicrap et al. [2014], Akroun et al. [2019]), no update locking of weights (Czarnecki et al. [2017], Jaderberg et al. [2017]), complete local Hebbian learning (Bengio et al. [2016], Whittington and Bogacz [2019]), single forward pass with no storage of activations single weight update per sample, and neural priors (in the

form of embedded vectors). As a consequence, SPELA can be a perfect candidate for perceptual representation learning studies which require both sensory input and priors (Kok et al. [2013], Hardstone et al. [2021], Brod et al. [2013], Summerfield and Koechlin [2008]) and hence makes a backpropagation-trained network unsuitable. Unlike most of the previously proposed biologically plausible algorithms, we here explicitly demonstrate the nonlinear classification power of SPELA as part of experiments of boolean (AND, OR, XOR) operations. Remarkably, SPELA achieves this without relying on a hidden layer, a direct connection from the input layer to the output layer with just two neurons is sufficient. It is observed that SPELA can learn without the need for neuron *bias* and a very high test-to-train ratio, which we also justify experimentally. Finally, we demonstrate the backpropagation equivalent generalization capacity of SPELA including on MNIST, KMNIST, and Fashion MNIST datasets. Under the few-shot one epoch regime, SPELA consistently outperforms backpropagation irrespective of the test-to-train split of data. During the classification of MNIST, KMNIST, and Fashion MNIST, SPELA can perform well despite a very high test-to-train ratio. We demonstrate that SPELA is also an optimal algorithm for training and inference under a resource-constrained AI application environment.

References

- Iliia Sucholutsky, Lukas Muttenthaler, Adrian Weller, Andi Peng, Andreea Bobu, Been Kim, Bradley C. Love, Erin Grant, Iris Groen, Jascha Achterberg, Joshua B. Tenenbaum, Katherine M. Collins, Katherine L. Hermann, Kerem Oktar, Klaus Greff, Martin N. Hebart, Nori Jacoby, Qiuyi Zhang, Raja Marjeh, Robert Geirhos, Sherol Chen, Simon Kornblith, Sunayana Rane, Talia Konkle, Thomas P. O’Connell, Thomas Unterthiner, Andrew K. Lampinen, Klaus-Robert Müller, Mariya Toneva, and Thomas L. Griffiths. Getting aligned on representational alignment, 2023.
- Christopher Summerfield and Etienne Koechlin. A neural representation of prior information during perceptual inference. *Neuron*, 59(2):336–347, July 2008.
- Jeffrey R Binder, Rutvik H Desai, William W Graves, and Lisa L Conant. Where is the semantic system? a critical review and meta-analysis of 120 functional neuroimaging studies. *Cereb Cortex*, 19(12):2767–2796, March 2009.
- Szu-Han Wang and Richard G.M. Morris. Hippocampal-neocortical interactions in memory formation, consolidation, and reconsolidation. *Annual Review of Psychology*, 61(1):49–79, 2010. doi:10.1146/annurev.psych.093008.100523. URL <https://doi.org/10.1146/annurev.psych.093008.100523>. PMID: 19575620.
- Peter Kok, Gijs Joost Brouwer, Marcel A.J. van Gerven, and Floris P. de Lange. Prior expectations bias sensory representations in visual cortex. *Journal of Neuroscience*, 33(41):16275–16284, 2013. ISSN 0270-6474. doi:10.1523/JNEUROSCI.0742-13.2013. URL <https://www.jneurosci.org/content/33/41/16275>.
- Richard Hardstone, Michael Zhu, Adeen Flinker, Lucia Melloni, Sasha Devore, Daniel Friedman, Patricia Dugan, Werner K. Doyle, Orrin Devinsky, and Biyu J. He. Long-term priors influence visual perception through recruitment of long-range feedback. *Nature Communications*, 12(1):6288, Nov 2021. ISSN 2041-1723. doi:10.1038/s41467-021-26544-w. URL <https://doi.org/10.1038/s41467-021-26544-w>.
- Garvin Brod, Markus Werkle-Bergner, and Yee Lee Shing. The influence of prior knowledge on memory: a developmental cognitive neuroscience perspective. *Front Behav Neurosci*, 7:139, October 2013.
- Jean Piaget. The child’s conception of the world. *Humana Mente*, 4(15):422–424, 1929.
- Fergus I.M. Craik and Robert S. Lockhart. Levels of processing: A framework for memory research. *Journal of Verbal Learning and Verbal Behavior*, 11(6):671–684, 1972. ISSN 0022-5371. doi:[https://doi.org/10.1016/S0022-5371\(72\)80001-X](https://doi.org/10.1016/S0022-5371(72)80001-X). URL <https://www.sciencedirect.com/science/article/pii/S002253717280001X>.
- John D. Bransford and Marcia K. Johnson. Contextual prerequisites for understanding: Some investigations of comprehension and recall. *Journal of Verbal Learning and Verbal Behavior*, 11(6):717–726, 1972. ISSN 0022-5371. doi:[https://doi.org/10.1016/S0022-5371\(72\)80006-9](https://doi.org/10.1016/S0022-5371(72)80006-9). URL <https://www.sciencedirect.com/science/article/pii/S0022537172800069>.
- Dharshan Kumaran, Jennifer J. Summerfield, Demis Hassabis, and Eleanor A. Maguire. Tracking the emergence of conceptual knowledge during human decision making. *Neuron*, 63(6):889–901, 2009. ISSN 0896-6273. doi:<https://doi.org/10.1016/j.neuron.2009.07.030>. URL <https://www.sciencedirect.com/science/article/pii/S0896627309006187>.
- Dharshan Kumaran, Hans Ludwig Melo, and Emrah Duzel. The emergence and representation of knowledge about social and nonsocial hierarchies. *Neuron*, 76(3):653–666, 2012. ISSN 0896-6273. doi:<https://doi.org/10.1016/j.neuron.2012.09.035>. URL <https://www.sciencedirect.com/science/article/pii/S0896627312008896>.

- Marlieke T R van Kesteren, Guillén Fernández, David G Norris, and Erno J Hermans. Persistent schema-dependent hippocampal-neocortical connectivity during memory encoding and postencoding rest in humans. *Proc Natl Acad Sci U S A*, 107(16):7550–7555, April 2010.
- Marlieke T.R. van Kesteren, Sarah F. Beul, Atsuko Takashima, Richard N. Henson, Dirk J. Ruiter, and Guillén Fernández. Differential roles for medial prefrontal and medial temporal cortices in schema-dependent encoding: From congruent to incongruent. *Neuropsychologia*, 51(12):2352–2359, 2013. ISSN 0028-3932. doi:<https://doi.org/10.1016/j.neuropsychologia.2013.05.027>. URL <https://www.sciencedirect.com/science/article/pii/S002839321300184X>. Special Issue on Functional Neuroimaging of Episodic Memory.
- Meenal V. Narkhede, Prashant P. Bartakke, and Mukul S. Sutaone. A review on weight initialization strategies for neural networks. *Artificial Intelligence Review*, 55(1):291–322, Jan 2022. ISSN 1573-7462. doi:10.1007/s10462-021-10033-z. URL <https://doi.org/10.1007/s10462-021-10033-z>.
- Yoshua Bengio, Dong-Hyun Lee, Jorg Bornschein, Thomas Mesnard, and Zhouhan Lin. Towards biologically plausible deep learning, 2016.
- Timothy P. Lillicrap, Daniel Cownden, Douglas B. Tweed, and Colin J. Akerman. Random synaptic feedback weights support error backpropagation for deep learning. *Nature Communications*, 7(1):13276, Nov 2016. ISSN 2041-1723. doi:10.1038/ncomms13276. URL <https://doi.org/10.1038/ncomms13276>.
- Blake A. Richards, Timothy P. Lillicrap, Philippe Beaudoin, Yoshua Bengio, Rafal Bogacz, Amelia Christensen, Claudia Clopath, Rui Ponte Costa, Archy de Berker, Surya Ganguli, Colleen J. Gillon, Danijar Hafner, Adam Kepecs, Nikolaus Kriegeskorte, Peter Latham, Grace W. Lindsay, Kenneth D. Miller, Richard Naud, Christopher C. Pack, Panayiota Poirazi, Pieter Roelfsema, João Sacramento, Andrew Saxe, Benjamin Scellier, Anna C. Schapiro, Walter Senn, Greg Wayne, Daniel Yamins, Friedemann Zenke, Joel Zylberberg, Denis Therien, and Konrad P. Kording. A deep learning framework for neuroscience. *Nature Neuroscience*, 22(11):1761–1770, Nov 2019. ISSN 1546-1726. doi:10.1038/s41593-019-0520-2. URL <https://doi.org/10.1038/s41593-019-0520-2>.
- James C.R. Whittington and Rafal Bogacz. Theories of error back-propagation in the brain. *Trends in Cognitive Sciences*, 23(3):235–250, 2019. ISSN 1364-6613. doi:<https://doi.org/10.1016/j.tics.2018.12.005>. URL <https://www.sciencedirect.com/science/article/pii/S1364661319300129>.
- Timothy P. Lillicrap, Daniel Cownden, Douglas B. Tweed, and Colin J. Akerman. Random feedback weights support learning in deep neural networks, 2014.
- Mohamed Akrouf, Collin Wilson, Peter Humphreys, Timothy Lillicrap, and Douglas B Tweed. Deep learning without weight transport. In H. Wallach, H. Larochelle, A. Beygelzimer, F. d'Alché-Buc, E. Fox, and R. Garnett, editors, *Advances in Neural Information Processing Systems*, volume 32. Curran Associates, Inc., 2019. URL https://proceedings.neurips.cc/paper_files/paper/2019/file/f387624df552cea2f369918c5e1e12bc-Paper.pdf.
- Wojciech Marian Czarnecki, Grzegorz Swirszcz, Max Jaderberg, Simon Osindero, Oriol Vinyals, and Koray Kavukcuoglu. Understanding synthetic gradients and decoupled neural interfaces. In *Proceedings of the 34th International Conference on Machine Learning - Volume 70, ICML'17*, page 904–912. JMLR.org, 2017.
- Max Jaderberg, Wojciech Marian Czarnecki, Simon Osindero, Oriol Vinyals, Alex Graves, David Silver, and Koray Kavukcuoglu. Decoupled neural interfaces using synthetic gradients. In Doina Precup and Yee Whye Teh, editors, *Proceedings of the 34th International Conference on Machine Learning*, volume 70 of *Proceedings of Machine Learning Research*, pages 1627–1635. PMLR, 06–11 Aug 2017. URL <https://proceedings.mlr.press/v70/jaderberg17a.html>.
- Yann LeCun, Yoshua Bengio, and Geoffrey Hinton. Deep learning. *Nature*, 521(7553):436–444, May 2015. ISSN 1476-4687. doi:10.1038/nature14539. URL <https://doi.org/10.1038/nature14539>.
- D. O. Hebb. *The organization of behavior; a neuropsychological theory*. The organization of behavior; a neuropsychological theory. Wiley, Oxford, England, 1949. Pages: xix, 335.
- Richard P. Heitz. The speed-accuracy tradeoff: history, physiology, methodology, and behavior. *Frontiers in Neuroscience*, 8, 2014. ISSN 1662-453X. doi:10.3389/fnins.2014.00150. URL <https://www.frontiersin.org/journals/neuroscience/articles/10.3389/fnins.2014.00150>.
- Marcin Penconek. Computational analysis of speed-accuracy tradeoff. *Scientific Reports*, 12(1):21995, Dec 2022. ISSN 2045-2322. doi:10.1038/s41598-022-26120-2. URL <https://doi.org/10.1038/s41598-022-26120-2>.
- Molly E. Zimmerman. *Speed–Accuracy Tradeoff*, pages 2344–2344. Springer New York, New York, NY, 2011. ISBN 978-0-387-79948-3. doi:10.1007/978-0-387-79948-3_1247. URL https://doi.org/10.1007/978-0-387-79948-3_1247.

- Anthony Zador, Sean Escola, Blake Richards, Bence Ölveczky, Yoshua Bengio, Kwabena Boahen, Matthew Botvinick, Dmitri Chklovskii, Anne Churchland, Claudia Clopath, James DiCarlo, Surya Ganguli, Jeff Hawkins, Konrad Kording, Alexei Koulikov, Yann LeCun, Timothy Lillicrap, Adam Marblestone, Bruno Olshausen, Alexandre Pouget, Cristina Savin, Terrence Sejnowski, Eero Simoncelli, Sara Solla, David Sussillo, Andreas S. Tolias, and Doris Tsao. Catalyzing next-generation artificial intelligence through neuroai. *Nature Communications*, 14(1):1597, Mar 2023. ISSN 2041-1723. doi:10.1038/s41467-023-37180-x. URL <https://doi.org/10.1038/s41467-023-37180-x>.
- Mike Davies, Narayan Srinivasa, Tsung-Han Lin, Gautham China, Yongqiang Cao, Sri Harsha Choday, Georgios Dimou, Prasad Joshi, Nabil Imam, Shweta Jain, Yuyun Liao, Chit-Kwan Lin, Andrew Lines, Ruokun Liu, Deepak Mathaikutty, Steven McCoy, Arnab Paul, Jonathan Tse, Guruguhanathan Venkataramanan, Yi-Hsin Weng, Andreas Wild, Yoonseok Yang, and Hong Wang. Loihi: A neuromorphic manycore processor with on-chip learning. *IEEE Micro*, 38(1):82–99, 2018. doi:10.1109/MM.2018.112130359.
- Dharmendra S. Modha, Filipp Akopyan, Alexander Andreopoulos, Rathinakumar Appuswamy, John V. Arthur, Andrew S. Cassidy, Pallab Datta, Michael V. DeBole, Steven K. Esser, Carlos Ortega Otero, Jun Sawada, Brian Taba, Arnon Amir, Deepika Bablani, Peter J. Carlson, Myron D. Flickner, Rajamohan Gandhasri, Guillaume J. Garreau, Megumi Ito, Jennifer L. Klamo, Jeffrey A. Kusnitz, Nathaniel J. McClatchey, Jeffrey L. McKinstry, Yutaka Nakamura, Tapan K. Nayak, William P. Risk, Kai Schleupen, Ben Shaw, Jay Sivagnaname, Daniel F. Smith, Ignacio Terrizzano, and Takanori Ueda. Neural inference at the frontier of energy, space, and time. *Science*, 382(6668):329–335, 2023. doi:10.1126/science.adh1174. URL <https://www.science.org/doi/abs/10.1126/science.adh1174>.
- Geoffrey Hinton. The forward-forward algorithm: Some preliminary investigations, 2022.
- Alexander Ororbia. Contrastive-signal-dependent plasticity: Forward-forward learning of spiking neural systems, 2023.
- Albert Gidon, Timothy Adam Zolnik, Pawel Fidzinski, Felix Bolduan, Athanasia Papoutsis, Panayiota Poirazi, Martin Holtkamp, Imre Vida, and Matthew Evan Larkum. Dendritic action potentials and computation in human layer 2/3 cortical neurons. *Science*, 367(6473):83–87, 2020. doi:10.1126/science.aax6239. URL <https://www.science.org/doi/abs/10.1126/science.aax6239>.
- Garrick Orchard, E. Paxon Frady, Daniel Ben Dayan Rubin, Sophia Sanborn, Sumit Bam Shrestha, Friedrich T. Sommer, and Mike Davies. Efficient neuromorphic signal processing with loihi 2, 2021.
- Cengiz Pehlevan. A spiking neural network with local learning rules derived from nonnegative similarity matching. In *ICASSP 2019 - 2019 IEEE International Conference on Acoustics, Speech and Signal Processing (ICASSP)*, pages 7958–7962, 2019. doi:10.1109/ICASSP.2019.8682290.
- Benjamin James Lansdell, Prashanth Ravi Prakash, and Konrad Paul Kording. Learning to solve the credit assignment problem. In *International Conference on Learning Representations*, 2020. URL <https://openreview.net/forum?id=ByeUBANtvB>.
- Fabio Giampaolo, Stefano Izzo, Edoardo Prezioso, and Francesco Piccialli. Investigating random variations of the forward-forward algorithm for training neural networks. In *2023 International Joint Conference on Neural Networks (IJCNN)*, pages 1–7, 2023. doi:10.1109/IJCNN54540.2023.10191727.
- Ben Sorscher, Surya Ganguli, and Haim Sompolinsky. Neural representational geometry underlies few-shot concept learning. *Proc Natl Acad Sci U S A*, 119(43):e2200800119, October 2022a.
- Ali Momeni, Babak Rahmani, Matthieu Malléjac, Philipp del Hougne, and Romain Fleury. Backpropagation-free training of deep physical neural networks. *Science*, 382(6676):1297–1303, 2023. doi:10.1126/science.adi8474. URL <https://www.science.org/doi/abs/10.1126/science.adi8474>.
- J. B. Kruskal. Multidimensional scaling by optimizing goodness of fit to a nonmetric hypothesis. *Psychometrika*, 29(1):1–27, Mar 1964. ISSN 1860-0980. doi:10.1007/BF02289565. URL <https://doi.org/10.1007/BF02289565>.
- Edward B Saff and Amo BJ Kuijlaars. Distributing many points on a sphere. *The mathematical intelligencer*, 19:5–11, 1997.
- Henry Cohn and Abhinav Kumar. Universally optimal distribution of points on spheres. *Journal of the American Mathematical Society*, 20(1):99–148, 2007.
- Georgia Dellaferrera and Gabriel Kreiman. Error-driven input modulation: Solving the credit assignment problem without a backward pass. In Kamalika Chaudhuri, Stefanie Jegelka, Le Song, Csaba Szepesvari, Gang Niu, and Sivan Sabato, editors, *Proceedings of the 39th International Conference on Machine Learning*, volume 162 of *Proceedings of Machine Learning Research*, pages 4937–4955. PMLR, 17–23 Jul 2022. URL <https://proceedings.mlr.press/v162/dellaferrera22a.html>.

- Danilo Pietro Pau and Fabrizio Maria Aymone. Suitability of forward-forward and pepita learning to mlcommons-tiny benchmarks. In *2023 IEEE International Conference on Omni-layer Intelligent Systems (COINS)*, pages 1–6, 2023. doi:10.1109/COINS57856.2023.10189239.
- Matthew Mithra Noel, Shubham Bharadwaj, Venkataraman Muthiah-Nakarajan, Praneet Dutta, and Geraldine Bessie Amali. Biologically inspired oscillating activation functions can bridge the performance gap between biological and artificial neurons, 2023.
- Juhyeon Kim, Emin Orhan, Kijung Yoon, and Xaq Pitkow. Two-argument activation functions learn soft xor operations like cortical neurons. *IEEE Access*, 10:58071–58080, 2022. doi:10.1109/ACCESS.2022.3178951.
- Charles B. Delahunt and J. Nathan Kutz. Putting a bug in ml: The moth olfactory network learns to read mnist. *Neural Networks*, 118:54–64, 2019. ISSN 0893-6080. doi:https://doi.org/10.1016/j.neunet.2019.05.012. URL <https://www.sciencedirect.com/science/article/pii/S0893608019301522>.
- Ilenna Simone Jones and Konrad Paul Kording. Can single neurons solve mnist? the computational power of biological dendritic trees, 2020.
- Linda B. Smith, Susan S. Jones, Barbara Landau, Lisa Gershkoff-Stowe, and Larissa Samuelson. Object name learning provides on-the-job training for attention. *Psychological Science*, 13(1):13–19, 2002. doi:10.1111/1467-9280.00403. URL <https://doi.org/10.1111/1467-9280.00403>. PMID: 11892773.
- Paul C Quinn, Peter D Eimas, and Stacey L Rosenkrantz. Evidence for representations of perceptually similar natural categories by 3-month-old and 4-month-old infants. *Perception*, 22(4):463–475, 1993. doi:10.1068/p220463. URL <https://doi.org/10.1068/p220463>. PMID: 8378134.
- Ananya Rastogi. Learning about few-shot concept learning. *Nature Computational Science*, 2(11):698–698, Nov 2022. ISSN 2662-8457. doi:10.1038/s43588-022-00367-1. URL <https://doi.org/10.1038/s43588-022-00367-1>.
- Brenden M Lake, Ruslan Salakhutdinov, and Joshua B Tenenbaum. Human-level concept learning through probabilistic program induction. *Science*, 350(6266):1332–1338, 2015.
- Kaidi Cao, Maria Brbic, and Jure Leskovec. Concept learners for few-shot learning. In *International Conference on Learning Representations*, 2021. URL <https://openreview.net/forum?id=eJIJF3-LoZ0>.
- Ben Sorscher, Surya Ganguli, and Haim Sompolinsky. Neural representational geometry underlies few-shot concept learning. *Proc Natl Acad Sci U S A*, 119(43):e2200800119, October 2022b.